Development of a distributed OBDH system with MIL-STD-1553B and its application[1]

Joonyun Kim and Jungyoup Han
Korea Aerospace Research Institute
P.O.Box 113 Yusung
Taejon 305-600
Republic of Korea
+82-42-860-2462,2823
jnkim@kari.re.kr, coolboy@kari.re.kr

Abstract— This paper includes development of a distributed data processing system for both space mission vehicles and test results by ground experiment.

We developed test models of OBC(On Board Computer), RIU(Remote Interface Unit), and MIL-STD-1553B data bus to meet requirements of a space vehicle. OBC and RIU hardware specifications, memory size, number of channels, data acquisition frequency and CPU throughput are designed followed by quantitative analysis considering its mission requirements.

Tests of the developed systems were conducted with a satellite attitude control simulator to demonstrate their applicability on space mission vehicles. Experimental results show the developed system can be applied to space mission vehicles through further enhancement of performance in the future.

TABLE OF CONTENTS

1. INTRODUCTION

Current satellites and launch vehicles adopt microprocessor based systems as a OBDH(On Board Data Handling) system which processes tele-command and telemetry data, executes vehicle control, and manages subsystems. With growing demand of the OBDH's mission capability, the OBDH unit has become an essential part of space vehicles. Those on board computer systems have several features, such as radiation hardened technology, high reliability, fault tolerance, and high efficiency system.

Development of OBC, RIU and 1553B data bus is presented in this paper. OBC and RIU are designed and developed to meet space vehicle requirements. OBC hardware specification, memory size and CPU throughput are based on quantitative analysis considering its mission. MIL-STD-1553B is chosen as a communication data bus between subsystems because it has been proven with wide application in aerospace industry, for example, KOMPSAT(Korea Multi-Purpose Satellite) 1 and Koreasat 3 [1-3].

RIU stand alone test was executed with a satellite mockup testbed [4]. In addition to the test, OBC and RIU integration test through 1553B data bus was executed with the testbed also. Those experiments are addressed in this paper to prove that the system is capable of controlling a subsystem of space mission vehicle.

In general, a computer system of space mission vehicles has either distribution system or central digital system architecture. To implement fault tolerant system with ease we selected the distributed topology in this paper.

2. DEVELOPMENT OF MODULES

OBC

OBC's main functions of space mission system include housekeeping, health monitoring, system management, data transmission to ground segment, receiving and distribution of tele-commands to subsystems.

Our R&D's main objective is development of a distributed computer system for LEO satellites, GEO satellites, and/or launch vehicles. To design an embedded system on space mission, estimation of code size, memory size and throughput is carried out in advance. OBC hardware and software are developed followed by the result of quantitative estimation of code size, memory size and throughput [3]. Table 1 shows the estimation result of code size and throughput.

Based on the estimation, 80C186XL 12MHz, 64K ROM and 256K SRAM were chosen. 80C186 CPU has extensive heritages: KITSAT (Korea Institute of Technology Satellite) 1&2 employed it as primary processing processors. And KOMPSAT 1 uses it as a on board main processor, an AOCS(Attitude and Orbit Control System) processor and an EPS(Electrical Power System) processor.

PLD(Programmable Logic Devices) are used for I/O selection and signal generation of a passive backplane. A 3U VME module is adopted as internal data bus backplane. However the backplane pins are re-assigned suitable for a 16-bit dual processor control system as well as a 16/32-bit single processor system. And the OBC contains a serial interface for upload programming and download telemetry data and MIL-STD-1553B BC(Bus Controller) interface board for subsystem to subsystem communication.

Table 1. Estimation of code size and throughput

Code	Size	Throughput
Startup Code	5K	20KIPS
Executive	20K	160KIPS
TC&R	10K	80KIPS
Fault Management	10K	20KIPS
Attitude Control	20K	320KIPS
RTOS Kernel	2K	N.A.
Total	67K	600KIPS

KIPS: Kilo Instructions Per Second

RIU

RIU's functions are categorized by two major functions which are tele-data processing and control of subsystems. Tele-data processing task includes telemetry function and tele-command function. Telemetry functions cover telemetry gathering, formatting, and transmission. Tele-command functions cover receiving telemetry data from an OBC, and execution the received tele-commands. Control tasks depend on their applications, for example, power control, valve drive control, and so on.

Table 2. Key features of RIU I/O boards

Components	Features
Analog DAC	
Max sample rate	25KHz
Channels and resolution	32 channels, 12bit
Input Ranges	-/+10V, -/+5V, 0 ~ 10V
Expandability	Additional 32 channels
Analog Driver	
Channels and resolution	8 channels, 12 bit
Output Ranges	-/+10V, -/+5V, 0 ~ 10V
Expandability	Additional 8 channels
Digital I/O	
Input channels	16 channels
Output channels	16 channels
Expandability	Additional 16 channels respectively

RIU has a main board, an analog data acquisition board, an analog voltage driver board, a digital I/O board, and a MIL-STD-1553B RT data bus board. Table 2 shows key features of RIU I/O boards. As shown in Table 2, RIU I/O boards possess not only typical features of I/O boards but also flexible expandability to accommodate future needs.

MIL-STD-1553B Data Bus

Since MIL-STD-1553B data bus has been adopted as a standard data bus in aerospace industry, it has been regarded as the most generally used data bus in aircraft, weapon systems, and spacecraft.

There are many devices supporting the MIL-STD-1553B data bus. Among many MIL-STD-1553B devices, ILCDDC 61580 ACE (Advanced Communication Engine) is selected as a BC, a RT, and a MT (Monitor) device. It can support 3 types of terminals by programming. In addition, it contains 4K words of internal buffered RAM being run by only +5V. Interface between CPU and MIL-STD-1553B device is realized by 16-bit buffered mode [6].

3. EXPERIMENTAL TESTS

Single axis rotational testbed(a satellite attitude mockup system)

A satellite attitude control experimental mockup system, a single axis rotational testbed is developed and used to verify the RIU functions. Figure 1 shows the hardware interface configuration between the RIU and the single axis rotational testbed.

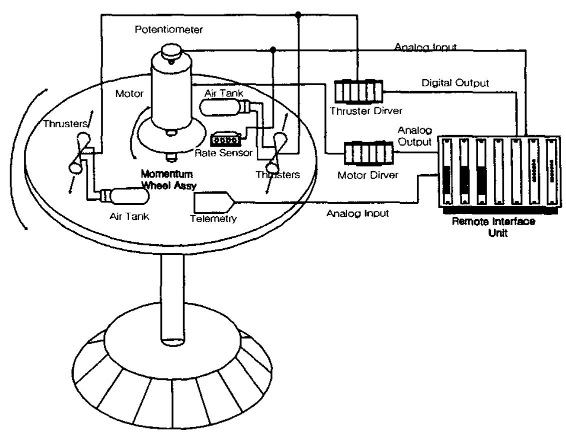

Fig. 1 Hardware configuration of RIU and testbed

There is a rotating round table on the top of a single axis bearing which connects the rotational part to the stationary post. A reaction wheel and its driving motor are on the center of the table. Two thrusters and air tanks are symmetrically on the sides of the table. The sensor system consists of a tachometer measuring the speed of the reaction wheel, a potentiometer, and an angular velocity sensor measuring its angular rate. The RIU is used as a controller to acquire sensing data, to drive the motor, and to compute control signals.

Made of aluminum (A6061), the round table is light and easy-to-treat. A Taper roll bearing is used to minimize friction force. The momentum of inertia of the single axis testbed system and the reaction wheel is $2.32\,\mathrm{kgm}^2$ and $93\times10^{-3}\,\mathrm{kgm}^2$, respectively. The output level of the thrusters is measured about 0.587Nm.

Detailed specifications of the single axis rotational testbed used in this study are shown in Table 3.

Table 3 Specifications of the single axis rotational testbed

DC Servo Motor
Max. speed – 5000rpm, weight - 2.4kg
Air Tank
Radius/height - 5.5/40cm, max. pressure - 3000psi
Solenoid Valve
Op. voltage – 24V, Op. pressure - 200psi
Regulator
Input pressure : 3000psi, Output pressure : 100psi
Potentiometer
Op. voltage – 14V, Sensitivity - 0.05 °
Power Module
Output Voltage - ±72V, Output Current - ±3A
Loop Gain - 7.2V/V & 0.3A/V
Rate Sensor
Input Voltage - ±15V, Output - ±10V
Scales – 3 °/sec/volt

Figures 2 and 3 show the thrusters, air tank, the reaction wheel attached to the driving motor.

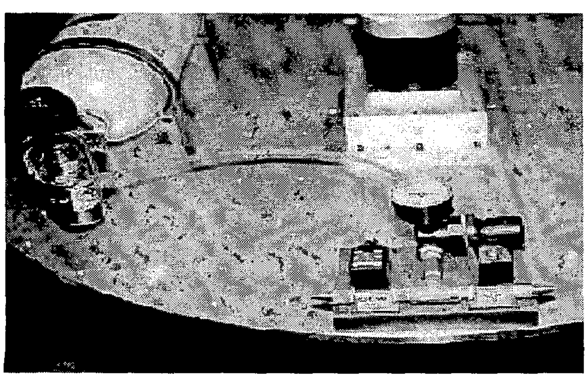

Fig. 2 Photograph of the thrusters and the air tank

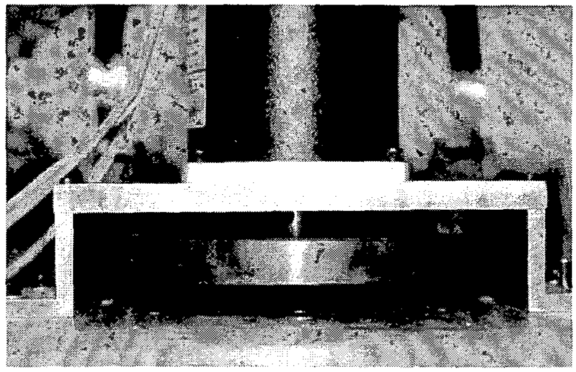

Fig. 3 Photograph of the reaction wheel with the motor

RIU Stand-alone Test

Figure 4 shows a control block diagram used for this experimental study. The rotational testbed system is depicted as spacecraft. RWA (Reaction Wheel Assembly) is represented by the reaction wheel, the driving motor, and a voltage amplifier.

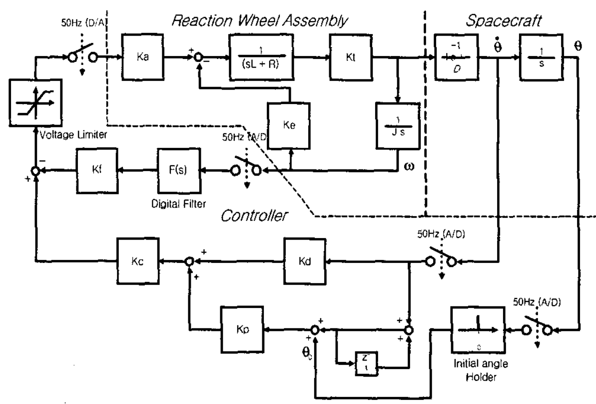

Fig. 4 Control block diagram

To emulate ESA (Earth Sensor Assembly) and gyros, the potentiometer and the rate sensor is used to acquire the initial attitude and angular rate error signals, respectively. And a proportional plus derivative (PD) controller is adopted to feedback angular attitude and rate error.

Mathematical representations of spacecraft, Reaction Wheel Assembly, and the controller are as follows:

Spacecraft:

$$J\dot{\omega} = I\ddot{\theta} + D\dot{\theta} \tag{1}$$

Reaction Wheel Assembly:

$$JL\ddot{\omega} + RJ\dot{\omega} + K_t K_e \omega = K_t K_a u \tag{2}$$

Controller:

$$u = K_c(K_p\theta + K_d\dot{\theta}) - K_f\omega \tag{3}$$

Table 4 shows satellite mockup system parameters and values used in this study.

Table 4 Satellite attitude mockup system parameters and values

Thruster	
Thruster Torque, N	0.587Nm
Reaction Wheel Assembly	
Armature Inductance, L	2.7mH
Armature Resistance, R	$1\,\Omega$
Armature Inertia	1.6×10^{-4}kgm^2
Torque Constant, K_t	0.1Nm/A
Back EMF Constant, K_e	0.1V/rad/sec
Amp Gain, K_a	7.2V/V
Reaction Wheel Inertia, J	4.93×10^{-3}kgm^2
Spacecraft	
Spacecraft Inertia, I	2.32 kgm^2
Proportional-Derivative Controller	
Proportional Gain, $K_c \times K_p$	300×75
Derivative Gain, $K_c \times K_d$	300×30
Tachometer Feedback Gain, K_f	1V/rad/sec
Voltage Output Limits	± 9.9V
Digital Filter Gain	1V/V
Digital Filter Lag	0.3sec

Assuming only the initial attitude error of 14°, simulation results using the PD controller, and parameters in Table 4 are presented in Fig. 5. The initial angular attitude error is nearly eliminated after about 2.5sec.

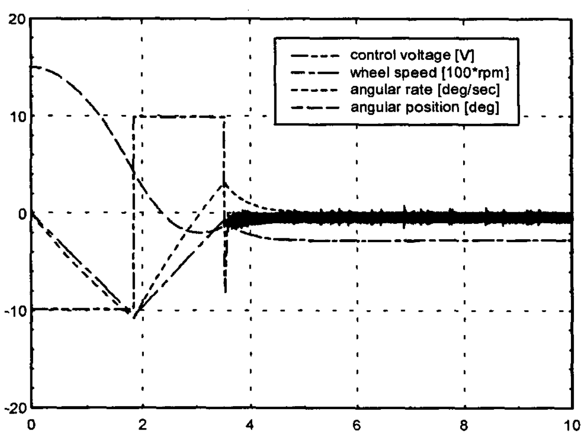

Fig 5 Simulation result for RIU stand-alone test

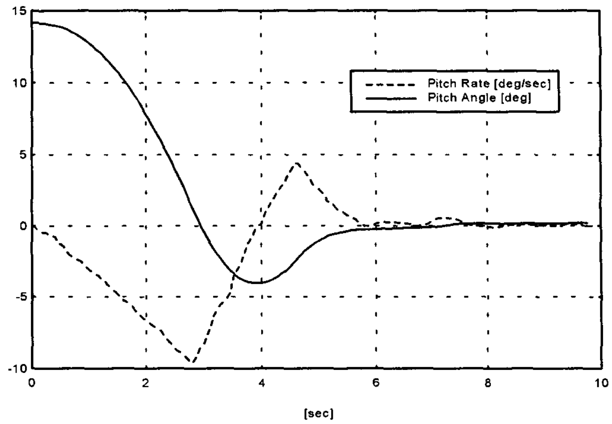

Fig. 6 Experimental result of RIU stand-alone test

Integration Test

The performance of the developed system has been studied with integration test. RIU is interfaced with the OBC through 1553B data bus. As shown in Fig. 1, the testbed configuration is used also except RWA replaced with thrusters. Thrusters are placed symmetrically on the rotational table, the one clock-wise thruster and the other counter clock-wise thruster.

The time-optimal attitude controller is employed for the integration test. It is a well known bang-bang profile for a simple rigid body. The single switching takes place at the half maneuver time. Neglecting a damping term in the single axis rotational testbed, the governing equation of the system is as following:

$$I\ddot{\theta} = u(t), \qquad |u(t)| = N \tag{4}$$

Where $u(t)$ is a control torque applied to the system and N is the magnitude of the applied torque by the on-off thrusters. The closed-loop time-optimal control law is

$$u(t) = -N \times sign\{(\theta - \theta_f) + \frac{I}{2N}\dot{\theta}\,|\,\dot{\theta}\,|\} \tag{5}$$

where $sign(f)$ (1 if $f > 0$ and -1 if $f < 0$) is a sign function determining the control torque direction. The θ_f is the final desired angular attitude to be reached.

Figure 7 shows the simulation result by application of the time-optimal controller. It takes 0.02sec(50Hz) from data acquisition, transmit, calculation, to the execution of command. These functions are executed concurrently at OBC and RIU. Data acquisition module samples 10 data and transmits average values to minimize noise effect. OBC receives the acquisition data and calculates the position error value. After computation of the error, OBC send a command whether clockwise ON, counter-clockwise ON or both off.

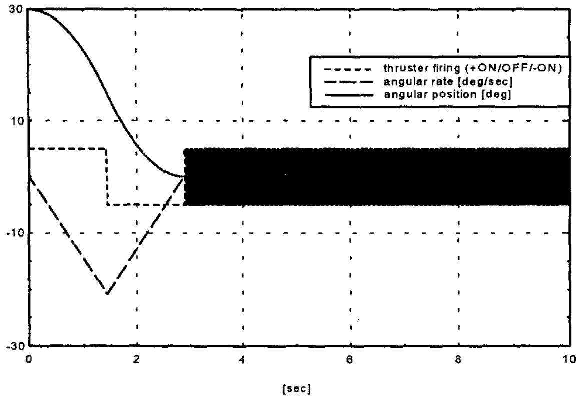

Fig. 7 Time-optimal simulation result for integration test

Figure 8 shows hardware interface of the integration test. OBC contains 1553B data bus controller and its terminal address is 0x00. RIU works as a remote terminal whose terminal address is 0x01. And monitoring PC gathers 1553B data and stores the data in magnetic storage.

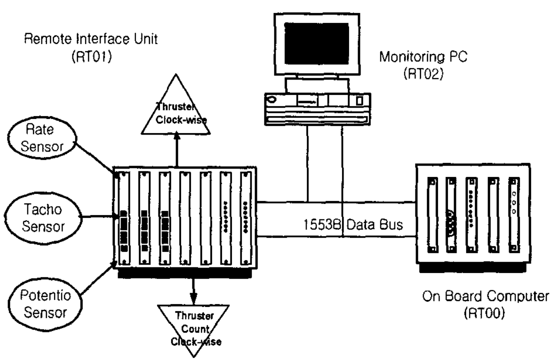

Fig. 8 Hardware interface block diagram of integration test

Figure 9 shows message frame used during the integration test. The averaged angle and rate data are stored in sub-address 0x01 and 0x02 within RT memory. The tele-command from OBC is stored in sub-address 0x03 within RT memory.

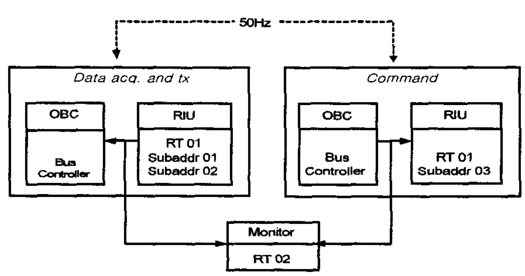

Fig. 9 Message frame of the integration test

Figure 10 shows experimental result of the integration test. An initial attitude error is decreased by thruster control in conjunction with the total system integrated.

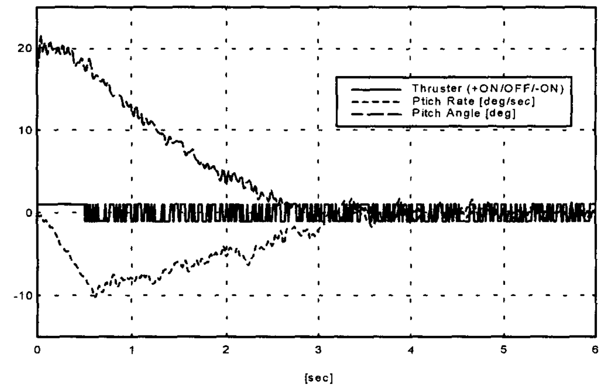

Fig. 10 Experimental result of integration test

4. CONCLUSIONS

This paper describes the first distributed OBDH system developed in the Republic of Korea.

RIU stand alone test and integration test were performed with a satellite mockup system. Experimental results show that the developed systems are capable of functioning properly on spacecraft mission applications.

The developed system may be targeted to other potential applications to sounding rockets, satellites and relevant ground systems.

ACKNOWLEDGEMENT

Much of the work has been supported by Korea Telecom and the support is very appreciated. And the authors express their sincere thanks to members of Koreasat Group and Sounding Rocket Development Group in Korea Aerospace Research Institute.

REFERENCES

[1] Lockheed Martin, *Koreasat 3 CDR*, Lockheed Martin, 1998

[2] KARI, *Development of Telemetry, Telecommand and Ranging System in Korea Multi-Purpose Satellite*, MOST, 1995

[3] W.J. Larson and J.R. Wertz, *Space Mission Analysis and Design*, Space Technology Library, 1992

[4] Jungyoup Han, Y.W. Park, H.C. Bang, and H. Hwangbo, "An experimental Study on Attitude Control of Spacecraft using Single Axis Rotational Simulation", *Korea Aerospace Society Journal 4, 83-91*, July 1998

[5] H.S. Kim, H.K. Lee and S.D. Choi, "On-Board Computer System for KITSAT-1 and 2," *Korea Space Science Society Special Edition*, S41-S51, December 1996

[6] ILCDDC, *Advance Communication Engine Integrated 1553 Terminal BU-61580 User's Guide*, ILCDDC, 1995

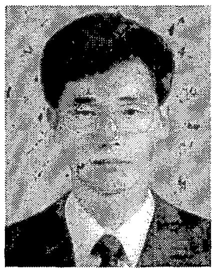

Joonyun Kim received the B.E. and M.S. degrees in Electronic Engineering from Kyungpook National University in 1992 and 1995, respectively. He joined Korea Aerospace Research Institute (KARI) in 1995, and had been engaged in Koreanization of OBDH system and MIL-STD-1553B data bus system. His current research interests include high performance on-board computer, high speed data bus and low cost and high reliability digital avionics system.

Jungyoup Han received his B.E. and M.E. in Control and Instrumentation Engineering from Korea University in 1994 and 1996, respectively. Since 1996 he had worked in Koreasat Group in Korea Aerospace Research Institute. He was a member of the team that designed and developed software and hardware for guidance, navigation and control system of a communication satellite. He is currently one of a responsible design engineer in AOCS team of Satellite Bus Dept. in Korea Aerospace Research Institute.

Laboratories). He is a senior member of the IEEE and has served as chairman of the VLSI for Signal Processing Technical Committee, and as a member of IEEE Neural Networks Council. His interests include digital signal processing, pattern recognition, neural and Bayesian networks.

Don Thompson is a member of IEEE holding a Ph.D. in mathematics from the University of Arizona (1979). He currently is in his twenty-first year as a member of the faculty of Pepperdine University, where he has taught mathematics and computer science. For the last three years he has served as the Associate Dean of Pepperdine's undergraduate school, overseeing curriculum, assessment, and technology efforts. His research interests belong with signal processing algorithms, neural network rule extraction, and Bayesian network modeling.

APPENDIX

Proof of Theorem 1:
The proof follows inductively on the number of components. The root case of one component follows.

First of all, it is clear that from our given information we may calculate P(C'), P(C'|T), and P(C'|T'): P(C') = 1 – P(C), P(C'|T) = 1- P(C|T), and P(C'|T') = 1-P(C|T'). Next, using the laws of probability we have:
P(C|T) = P(C,T)/P(T) = P(C,T)/(P(C,T) + P(C',T)) and P(C|T') = P(C,T')/P(T') = (P(C) - P(C,T))/(1- P(C,T) - P(C',T)). Solving for P(C,T), and P(C',T) we see that are led to the matrix system:

$$\begin{bmatrix} P(C'\mid T) & -P(C\mid T) \\ P(C'\mid T') & -P(C\mid T') \end{bmatrix}\begin{bmatrix} P(C,T) \\ P(C',T) \end{bmatrix} = \begin{bmatrix} 0 \\ P(C)-P(C\mid T') \end{bmatrix}$$

The determinant of the coefficient matrix of this system reduces to:

P(C|T)P(C'|T') – P(C'|T)P(C|T')

= P(C,T)P(C',T')-P(C',T)P(C,T')/(P(T)P(T')),

which has a vanishing numerator only if P(C,T)/P(C',T) = P(C,T')/P(C',T'), which is equivalent to C and T being independent events. We assume that this is not the case, else our conditional probabilities all collapse to prior probabilities, an uninteresting case.

Upon solving the above matrix system, we get P(C,T) and P(C',T); hence also P(C,T') = P(C) – P(C,T) and P(C',T') = P(C') – P(C',T). Thus, we can complete determine the joint distribution of C and T. This will uniquely determine all pertinent probabilities in this two-node network, including the causal probabilities.

The general case follows in a similar manner.
Q.E.D.